

## Article

# Evaluation of Cost-Effective Modified Binder Thin Chip and Cape Seal Surfacing on an Anionic Nano-Modified Emulsion (NME)-Stabilised Base Layer Using Accelerated Pavement Testing (APT)

Gerrit J. Jordaan <sup>1,2,\*</sup> , Wynand J. vd M. Steyn <sup>3</sup>  and Andre Broekman <sup>1</sup> <sup>1</sup> Department of Civil Engineering, University of Pretoria, Pretoria 0002, South Africa; andre@broekmail.com<sup>2</sup> Jordaan Professional Services (Pty) Ltd., Pretoria 0062, South Africa<sup>3</sup> Department of Civil Engineering & School of Engineering, University of Pretoria, Pretoria 0002, South Africa; Wynand.steyn@up.ac.za

\* Correspondence: jordaangj@tshepega.co.za; Tel.: +27-824164945

**Featured Application:** The surfacing layer on roads plays an essential role in the future performance of the road structure. In many traditional design approaches, the surfacing is also the most expensive part of the road pavement structure. It is directly exposed to the traffic loading as well as to often, harsh environmental conditions. The performance of the surfacing is highly dependent on the characteristics of the binder used and the interaction of the surfacing with the environment and the rest of the pavement structure. New-age nanotechnologies enable engineers to use modify binders to substantially improve the performance of surfacings and reduce the thicknesses thereof without compromising the integrity of the road structure as a whole. The optimisation of binder characteristics using applicable thin (chip seal) surfacings can contribute substantially to a reduction in road unit costs.

**Abstract:** Emulsion stabilisation of base layers surfaced with chip seals often proves problematic, with chips punching into the base and early distress. This can be aggravated by the use of modified binders that restricts the evaporation of moisture from pavement layers. The introduction of new-age (nano)-modified emulsion (NME) stabilisation has the advantage that water is chemically repelled from the stabilised layer, resulting in an accelerated development of strength. A need was identified to evaluate the early-life performance of selected chip and Cape seals, together with identified modified binders on anionic NME-stabilised base layers constructed with materials traditionally classified as unsuitable, using archaic empirically derived tests. Three different chip seal surfacings with unconventional modified binders were constructed and evaluated using accelerated pavement testing (APT) with the Model Mobile Load Simulator—3rd model (MMLS3). The objectives of the experimental design and testing were to evaluate the binder performance, chip seal performance in terms of early loss of chips before chip orientation, punching of the chips into the anionic NME-stabilised base and deformation characteristics of a Cape seal that was hand-laid using an anionic NME slurry without any cement filler. It was shown that that chip seal surfacings can be used at low risk, on a base layer containing materials with fines exceeding 22%. The selection of specific modified binders can reduce risks associated with chip seal surfacings, which can impact construction limitations. The recommended use of elastomer-modified binders on newly constructed or rehabilitated layers, resulting in moisture entrapment, needs to be reconsidered.

**Keywords:** nanotechnology; pavement engineering; chip seal surfacings; Cape seals; new-age modified emulsion (NME) stabilisation; anionic new-age modified emulsion slurries; modified binders; Sasobit-M<sup>®</sup> modified binders; accelerated pavement testing (APT); MMLS3



**Citation:** Jordaan, G.J.; Steyn, W.J.v.M.; Broekman, A. Evaluation of Cost-Effective Modified Binder Thin Chip and Cape Seal Surfacing on an Anionic Nano-Modified Emulsion (NME)-Stabilised Base Layer Using Accelerated Pavement Testing (APT). *Appl. Sci.* **2021**, *11*, 2514. <https://doi.org/10.3390/app11062514>

Academic Editors: Luis Picado Santos and Francesco Tornabene

Received: 26 January 2021

Accepted: 3 March 2021

Published: 11 March 2021

**Publisher's Note:** MDPI stays neutral with regard to jurisdictional claims in published maps and institutional affiliations.



**Copyright:** © 2021 by the authors. Licensee MDPI, Basel, Switzerland. This article is an open access article distributed under the terms and conditions of the Creative Commons Attribution (CC BY) license (<https://creativecommons.org/licenses/by/4.0/>).

## 1. Introduction

Surfaced road networks, creating accessibility to markets and reducing transportation costs, have been shown to be a major stimulus for economic growth. Developing areas around the world, such as sub-Saharan Africa, compares poorly with the developed world in terms of, *inter alia*, the percentage surfaced road network [1]. The general lack of adequate funding in developing regions, together with relatively high road unit construction costs, makes it almost impossible for these regions to provide the road network required to stimulate economic growth [2]. The high road unit construction costs are often associated with traditional use of material classification systems dating back many decades. These material classification systems generally exclude the use of naturally available materials in the upper load-bearing layers of a pavement structure [1]. Hence, high-quality, high-cost crushed stone, normally, has to be imported to construct road infrastructure. The material classification systems used, in many cases, are based on empirically derived tests, some dating back more than a century. These empirically derived tests were developed to limit the risks associated with the chemical weathering of materials and the formation of secondary minerals (e.g., clay) within the materials.

However, material-compatible nanotechnology solutions are able to neutralise any negative influence of secondary (or some primary) minerals. These technologies have been proven scientifically, in laboratories and in practice, using accelerated pavement testing (APT) with materials traditionally classified as marginal, or even unsuitable [1], stabilised with anionic New-age (nano) Modified Emulsions (NMEs) to be able to meet required engineering properties [3–5]. Enabling the use of naturally available materials in all structural road pavement layers can considerably reduce the construction costs of roads. However, to ensure success and limit the risks associated with the introduction of new technologies, implementation needs to be based on sound, scientifically based principles and fundamental engineering design methods [6–8].

To fully realise cost savings, the anionic NME-stabilised naturally available materials in the upper pavement layers must be suitable for use with relatively thin, durable surfacings such as various chip seals. The cost-effectiveness of these surfacings has been proven on roads constructed with traditionally classified materials all over the world, e.g., [9,10]. However, the traditional use of bitumen emulsion stabilisation in base layers, together with thin chip seal surfacings, has often proved problematic, with punching of the stone into the base. This leads to early distress in terms of severe bleeding of the binder, associated with rut deformation and early failure of the top of the base layer. These failures are invariably associated with high moisture build-up just below the surfacing, which can also result in detachment of the surfacing. With traditional emulsion stabilisation, moisture is only relieved from the layer through evaporation. The general specification and use of some modified binders known to restrict the evaporation of moisture from base and sub-base layers [11] entraps moisture and increases the risk of moisture build-up underneath the surfacing. This problem is not only restricted to emulsion-treated layers but also can be associated with any base and sub-base layer that will release moisture directly after construction, before reaching a state of equilibrium, such as granular and/or cemented layers. An equilibrium state within pavement layers is usually only reached after one to two seasons under traffic loading.

The introduction of material-compatible anionic NME stabilisation has the advantage that over and above evaporation, water is effectively repelled from the stabilised layer through a chemical reaction between the minerals of the materials and the material-compatible modifying agent applied to the emulsion. This results in accelerated drying of the layer, with an associated accelerated development of compressive and tensile strengths [6–8] and a reduced risk of early-life failures. It follows that the use of thin surfacings may be a cost-effective, low-risk option when used in combination with anionic NME-stabilised base layers and applicable modified binders. However, the cost-effectiveness of anionic NME stabilisation is directly related to the use of naturally available materials, traditionally classified as sub-standard or unsuitable [1,6] for use in the base/sub-base

layers of pavements. Logically, the use of such materials may increase the risk of early-life failure when used in combination with thin chip seal surfacings, given past experiences with unmodified bitumen emulsion stabilisation.

Hence, a need was identified to evaluate the early life of thin chip seal surfacings on a pavement constructed with an anionic NME-stabilised base layer using naturally available materials traditionally classified as unsuitable. It was realised that a proof of concept is required to address concerns about the risks associated with the use of chip seal surfacings on anionic NME-stabilised naturally available materials. In addition, successful validation of the viability of thin chip seal surfacings on such pavement layers will further contribute to the lowering of unit costs for the surfacing of gravel roads. Consequently, three test sections were constructed with three different types of chip seal surfacings. These seal types were specifically designed to address concerns about early-life failure.

The opportunity was also used to evaluate the impact of some novel binder modifications in combination with traditionally modified binders in the construction, testing and evaluation of the early-life performance of these chip seals. Considerable work has been done all over the world in the evaluation of various nanotechnologies on binders and asphalt behaviour [12,13]. However, little has previously been done to determine the effect of these technologies on thin chip seal surfacings.

The evaluation was done using high-speed, high-frequency, high-impact APT loading equipment, specifically designed to evaluate the deformation characteristics of asphalt layers for highways [14,15]. Due to the high-speed loading, it was deemed particularly suitable to evaluate possible punching of the chips (stone) into the base layer as well as to evaluate any deformation that may occur within the test area relative to the unloaded area.

High-accuracy, 3D scanning techniques based on Visual Simultaneous Localization and Mapping (VSLAM) [16] were used to quantify and evaluate possible aggregate loss, reorientation of the stone and punching of the stone into the base during APT. These 3D scans were done on areas subjected to APT loading and compared directly to adjacent unloaded areas to accurately quantify the performance of each seal. The digitised twin samples allowed for accurate objective calculations and analyses of the effect of APT loading on each of the different surfacings.

## 2. Materials Used in the Anionic NME-Stabilised Base Layer

It is not the objective of this paper to give a detailed description of the testing, evaluation and analysis done of the pavement design and the evaluation thereof in terms of the bearing capacity of the pavement structure. Of importance is an understanding of the materials used in the construction of the base (200 mm thick) directly on top of a sub-grade with a California Bearing Ratio (CBR) of <3 at 93% mod. AASHTO (modified CBR test as defined by the American Association of State and Highway Transportation Officials) [17–19] (which is basically a clay sub-grade) to form a highly flexible pavement structure. The naturally available materials used in the base were severely weathered material considered unsuitable for use in the upper pavement layers according to traditionally used material classifications (e.g., [20–22]).

The base layer was stabilised using 1.5% of a material-compatible anionic NME stabilising agent. The properties of the naturally available materials used for the construction of the base layer, mineralogy tests as well as the stabilised Unconfined Compressive Strength (UCS) and Indirect Tensile Strength (ITS) (test procedures described in [6]) are summarised in Figure 1. The laboratory-obtained engineering requirements can be compared to the material classification of NME4 as shown in Table 1 [7,23].

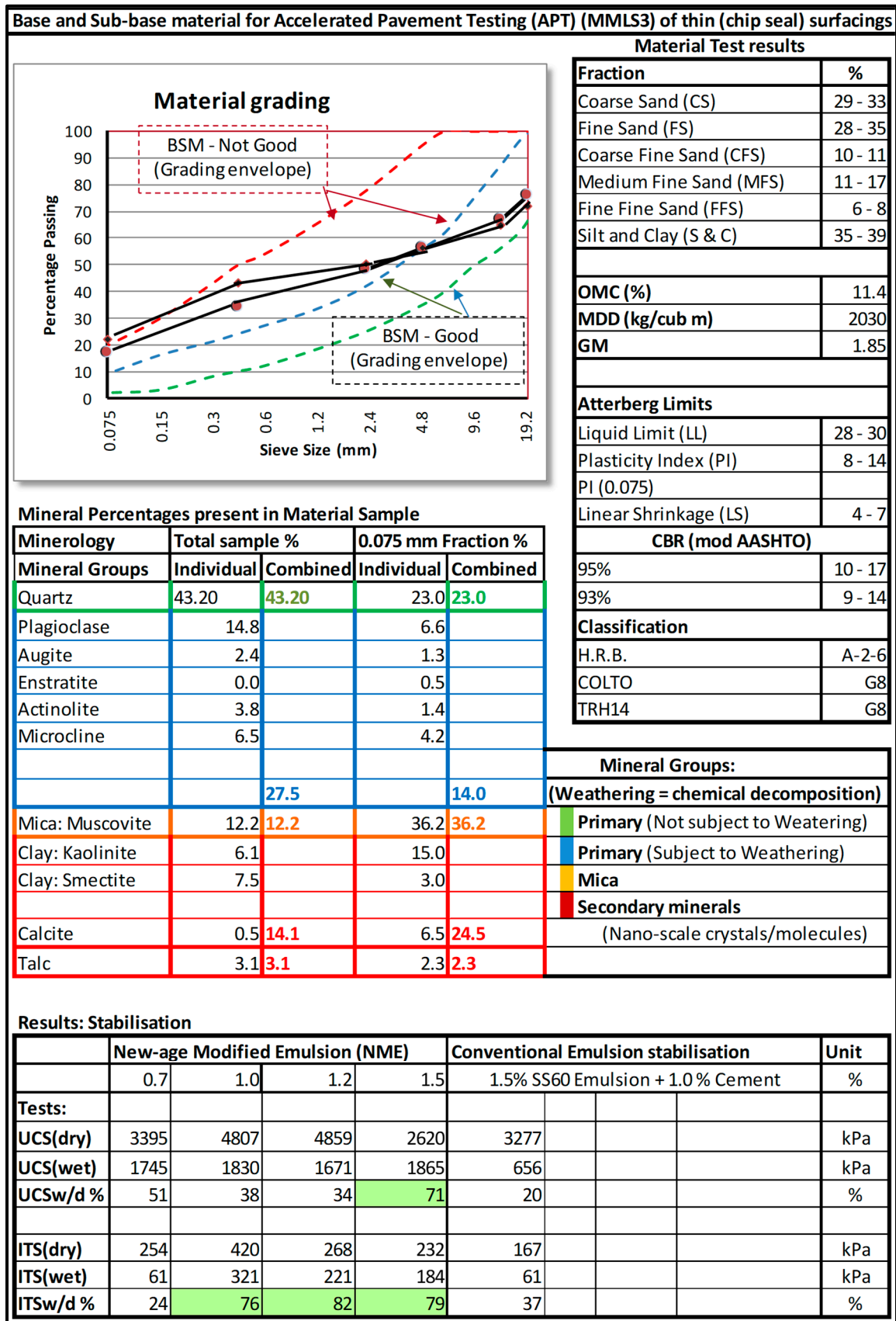


**Figure 1.** Material test results, mineralogy and new-age nano-modified emulsion (NME) stabilisation results of the base material. UCS, unconfined compressive strength; ITS, indirect tensile strength; BSM, bituminous stabilised materials.

**Table 1.** Engineering requirements for different material classifications [7,20].

Material <sup>1</sup>	Material Classification				
	NME1	NME2	NME3	NME4	
<b>Minimum material requirements before stabilisation and/or treatment (Natural materials)</b>					
Material <sup>1</sup> specifications (minimum)					
Un-stablished material: Soaked CBR <sup>2</sup> (%) (Mod. AASHTO)	CS/GS/NG/SSSC	>45 <sup>2</sup> (95%) ACV < 30%	>25 <sup>2</sup> (95%)	>10 <sup>2</sup> (93%)	>7 <sup>2</sup> (93%)
Grading Modulus (GM)	NG	>1.8	>1.5	-	-
Sieve analysis: % < 0.075 mm (P <sub>0.075</sub> )	ALL	<20%	<25%	<35%	<50%
XRD scans:					
- Total sample	ALL	✓	✓	✓	✓
- 0.075 mm fraction (P <sub>0.075</sub> )	ALL	✓	✓	✓	✓
NME stabilisation with micro-meter (µm) emulsion particle sizes					
% Material passing 2 µm (P <sub>0.002</sub> ) (e.g., Clay & Mica & Talc) as a % of Material (with Talc < 10%) (XRD-scans of the material passing the 0.075 mm sieve is used to determine the % clay, mica and talc in the material—In this case P <sub>0.002</sub> = P <sub>0.075</sub> × (P <sub>clay,etc.</sub> in P <sub>0.075</sub> ), or % Silt and Clay	ALL	<15%	<15%	<15%	<15%
NME stabilisation with emulsion containing micro-scale as well as nano-scale particles (adjusted according to material grading)					
	ALL	NA	<35%	<35%	<35%
NME stabilisation with emulsion containing nano-scale and pico-scale particles (grading adjustments) together with technologies addressing workability of materials on site					
	ALL	NA	NA	>35%	>35%
<b>Material specifications after stabilisation and/or treatment</b>					
In-situ density to be required after stabilisation and compaction (mod. AASHTO) (%) (minimum)	Base	>100%	>100%	>98%	>97%
	Sub-base	NA	>98%	>97%	>95%
DCP (DN mm/blow) (Quality control) (stabilised and compacted)		NA	NA	<2.6	<3.5
Mod. AASHTO density (%) (for laboratory testing)		>100%	>100%	>100%	>100%
* UCS <sub>wet</sub> (kPa) (150 mm Φ Sample)	<b>Design</b> <sup>3</sup>	>2500	>1500	>1000	>750
	<b>Construction</b> <sup>4</sup>	>2200	>1200 <sup>5</sup>	>700 <sup>5</sup>	>450 <sup>5</sup>
Retained Compressive Strength (RCS): (UCS <sub>wet</sub> /UCS <sub>dry</sub> ) (%)		>85	>75	>70	>65
RCS in relation to minimum UCS <sub>wet(criteria)</sub> (RCS <sub>effective</sub> ) (%)		>100	>100	>100	>100
* ITS <sub>wet</sub> (kPa) (150 mm Φ Sample)	<b>Design</b> <sup>3</sup>	>240	>200	>160	>120
	<b>Construction</b> <sup>4</sup>	>220	>180 <sup>5</sup>	>140 <sup>5</sup>	>100 <sup>5</sup>
Retained Tensile strength (RTS): ITS <sub>wet</sub> /ITS <sub>dry</sub> (%)		>85	>75	>70	>65
RTS in relation to minimum ITS <sub>wet(criteria)</sub> (RTS <sub>effective</sub> ) (%)		>100	>100	>100	>100

<sup>1</sup> CS—crushed stone; NG—natural gravel; GS—gravel soil, and SSSC—sand, silty sand, silt, clay; ACV—Aggregate Crushing Value; <sup>2</sup> CBR only used as reference to traditionally used test procedures as a broad first indicator; \* Definitions: (UCS = Unconfined Compressive Strength) (ITS = Indirect Tensile Strength); UCS<sub>dry</sub>; ITS<sub>dry</sub> = testing after rapid curing; UCS<sub>wet</sub>; ITS<sub>wet</sub> = testing after rapid curing and 4 h in water; (RCS<sub>effective</sub>) = (RCS × (UCS<sub>wet</sub>/UCS<sub>wet(criteria)</sub>)); (RTS<sub>effective</sub>) = ((RTS × (ITS<sub>wet</sub>/ITS<sub>wet(criteria)</sub>))); **Design** <sup>3</sup> = Minimum criteria to be met in the laboratory during the design phase; **Construction** <sup>4</sup> = Minimum criteria to be met during construction as part of quality control; <sup>5</sup> Criteria based on Technical Guideline TG2 [24].

The variation in material properties shown in Figure 1 is the variation found in several samples of the materials tested along the 250 m length of a 3.7-m-wide lane constructed next to the road. Similar materials stabilised with an anionic NME stabilising agent were used in the adjacent pavement structure to evaluate the bearing capacity of the pavement with different layer thicknesses (150 mm base and 150 mm sub-base), as reported

elsewhere [4,5]. In the sub-base of the pavement structure only 1% NME stabilising agent was used due to the considerably higher ITS results obtained both in the dry and wet tests. Of note, the measured UCS and ITS values obtained using materials of unsuitable quality, when stabilised with a material-compatible anionic NME stabilising agent, far exceed the engineering requirements of an NME4 layer (Table 1). These measurements were obtained using the applicable test protocols [6,23] (developed for the evaluation of new-age stabilising agents [7]) and indicate the rapid strength development that was achieved by using the NME stabilisation based on a mineralogy-design approach.

### 3. Selection and Construction of Thin Chip and Cape Seal Surfacing

#### 3.1. Selection of Surfacing

The test sections constructed consisted of a 20 mm single chip seal, a 20/7 mm double chip seal and a Cape seal consisting of a 20 mm chip seal with a slurry mix. The 20 mm single chip seal was selected with the objective to evaluate the possible punching of the chip stones into the base layer. The second application of the 7 mm chips on the double seal was done with a traditional elastomer-modified binder to observe the possible entrapment of moisture. The third chip seal constructed is a Cape seal, which is of particular importance due to its proven durability and applicability within an urban as well as a rural environment [25,26]. The application of the slurry mix of the Cape seal can be done using manual labour, which is of importance in the developing world, where high rates of unemployment are a norm rather than an exception. In many countries, labour-intensive construction procedures are considered of high importance in Public Works Programmes (PWP), including road construction projects.

The layout of the test section is shown in Figure 2.

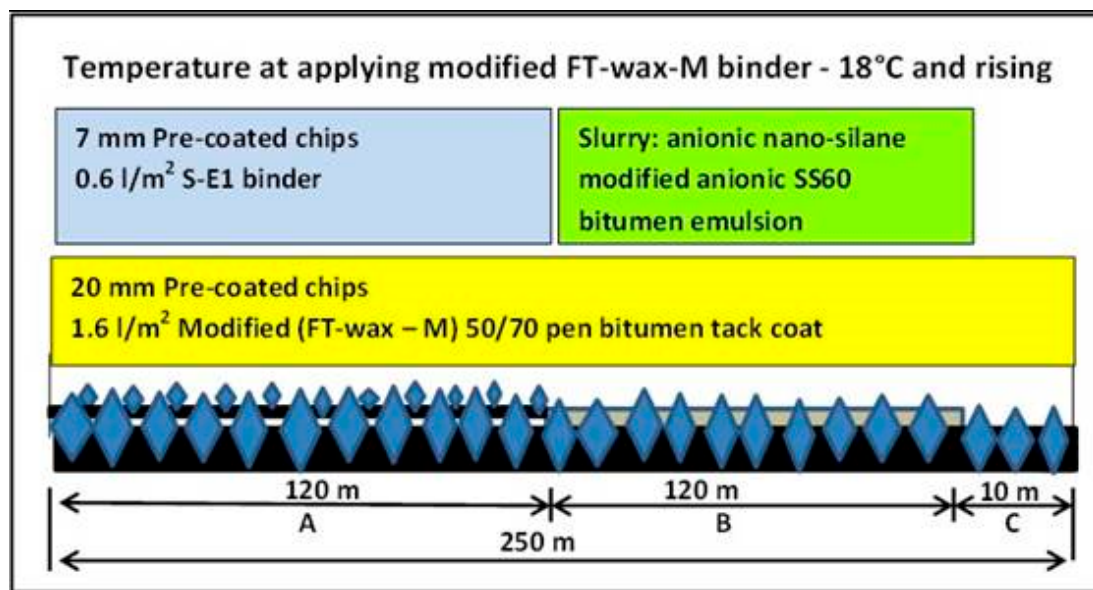


**Figure 2.** Experimental layout of three different chip and Cape seal surfacings constructed for Accelerated Pavement Testing (APT) and evaluation.

#### 3.2. Binder Selection

##### 3.2.1. General

Binder selection as part of any surfacing and the performance thereof in terms of the known parameters of the pavement structure are of importance. The early-life performance of thin chip seals is closely related to strict adherence to weather tolerances during construction (temperature and wet weather) [27,28]. It follows that the performance of thin chip seals is traditionally linked to good quality control during construction. Over and above

additional considerations, only the relevant data in terms of this paper are repeated in terms of road surface temperature requirements. According to best practice [27,28], binder application may only be placed under the following surface temperature conditions:

- Hot binders with 0% solvents: 25 °C and rising
- Emulsions: 10 °C and rising

The surface temperature can be reduced by 1 °C for each percentage point of a low flash-point solvent (LFS) (e.g., paraffin) added. For single and double seals with an elastomer-modified binder (S-E1 and S-E2) [11], a maximum of 4% LFS is recommended, while for a bitumen-rubber (S-R1) [11] binder, a maximum of 8% high flash-point solvent (HFS) is recommended.

Lower temperatures will normally lead to a rapid drop in binder temperatures, an increase in binder stiffness and a resultant increase in the risk of binder–chip adhesion failure [11]. Adhesion failure is the most common problem experienced with chip seals, with an associated risk during winter periods or under challenging construction conditions, resulting in a drop in binder temperature before spreading of the stone can be done. Trafficking of newly laid chip seals, before orientation of the stone has taken place at temperatures below 20 °C, will often also result in an increase in stone loss. It follows that any developments leading to the ease of construction tolerances will be beneficial for the successful use of chip seals under challenging conditions.

### 3.2.2. Binder Selection: Tack Coat for the First Application of the 20 mm Chips (Stone)

With the construction of the test sections on the anionic NME-stabilised base, binder options were considered with the specific intention to limit risks associated with construction and temperature-related aspects that could be challenging to meet under difficult construction and environmental conditions. The APT programme was inter alia, also designed to test at temperatures below 20 °C to evaluate stone loss during early trafficking while orientation of the stones took place. These aspects are not covered in this paper and are fully addressed elsewhere [29].

Conventional modified binders commonly used in the construction of chip seals do not allow for lowering of the temperature criteria, as stated above. In addition, an elastomer-modified binder has a disadvantage that it “can” or “does restrict the evaporation of moisture” [11] from a newly constructed base layer. This could result in moisture build-up underneath the surfacing and failures, as discussed. Hence, any unconventional modified binder must, over and above all the other considerations, also allow moisture evaporation to continue until a state of moisture equilibrium has been reached within the pavement layers (which usually takes at least two seasons under trafficking to occur).

SASOBIT<sup>®</sup> (Fischer-Tropsch (FT)) wax modifications [30] to bituminous binders were developed more than 25 years ago with well-known advantages, as confirmed all over the world (e.g., [31–33]). These advantages included the compaction of asphalt at temperatures as low as 80–90 °C (compared to unmodified binders, where a minimum of 120 °C is the norm). The original formulation of SASOBIT<sup>®</sup> has recently been improved, with a crude-oil additive to allow for compaction at temperatures as low as 60 °C. This new formulation is known as SASOBIT-M<sup>®</sup> [34], which also prevents an increase in viscosity at lower temperatures (associated with SASOBIT<sup>®</sup>). The comparison between the viscosities and compaction end temperatures of standard bitumen, 3% SASOBIT<sup>®</sup>-modified bitumen and 1.5% SASOBIT-M<sup>®</sup>-modified bitumen is demonstrated in Figure 3.

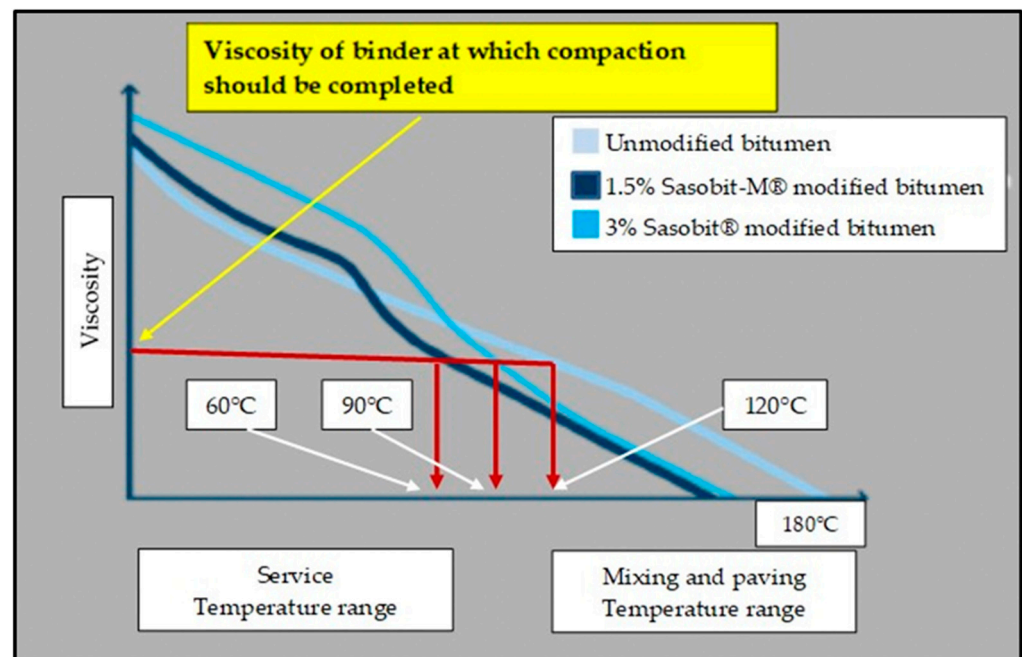


**Figure 3.** Working principles as applicable to a standard pen bitumen, 1.5% SASOBIT-M<sup>®</sup>-modified bitumen and 3% SASOBIT<sup>®</sup>-modified bitumen binder.

Logically, if the use of SASOBIT-M<sup>®</sup> allows for the lowering of compaction temperatures in asphalt, the same principle should also be applicable when used in a tack coat for the construction of chip seals, allowing for the placement of the chips at lower temperatures. If proved in practice, this modification will allow for chip seal surfacings to proceed at temperatures considerably lower than currently used specifications, without any negative effects (such as chip loss). Hence, contractors would also have more time to apply chips during the construction of seals without an increase in the risk of failures. Consequently, it was decided to use a tack coat consisting of a 60/70 pen bitumen modified with 1.5% SASOBIT-M<sup>®</sup> for the 20 mm chip seal. This tack coat was placed at an application rate of 1.6 L/m<sup>2</sup> at a surface temperature of 18 °C and rising (compared to the minimum specification of 25 °C and rising). These experimental sections are the first where Sasobit-M<sup>®</sup> modification has been used in the construction of chip seals.

### 3.2.3. Binder Selection: Second Binder Application for the Double Chip Seal

The binder selection for the placement of the second layer of the double seal (7 mm chips on top of the 20 mm chip seal) was aimed at the assessment of the performance of commonly used modified binders for chip seal applications on the anionic NME-stabilised base layer. Hence, a binder consisting of a 60/70 pen bitumen modified with an elastomer, i.e., a Styrene Butadiene Styrene (SBS) polymer (S-E2) [11], placed at 0.6 L/m<sup>2</sup>, was selected and used for the placement of the 7 mm chips. This modified binder is often specified for use by engineers without considering the noted disadvantage that it “does restrict evaporation of entrapped moisture” [11]. The binder used for the second layer was chosen specifically to assess the effect of possible entrapment of moisture evaporating from the anionic NME-stabilised base.

### 3.2.4. Binder Selection: Slurry for the Construction of the Cape Seal

Cape seals [25] are normally constructed using a slurry consisting of a bitumen emulsion, crusher dust, sand and a cement filler. The slurry provides additional protection and acts as an adhesive, keeping the stone in place where the turning movement of vehicle tyres can potentially result in stone loss. Practical experience has shown that a well-

constructed Cape seal can be expected to have an advantage in terms of maintenance-free surfaced life [26] comparable to that of an asphalt layer at considerably less costs.

The use of a cement or lime filler as part of the slurry mix may result in a brittle mix, reducing the crack-free life of the slurry seal on a highly flexible pavement structure. In this case, it was decided to test a slurry using an anionic nano-silane-modified emulsion with no cement or lime filler. The nano-silane will replace the normal cement or lime filler, potentially increasing the crack-free life of the seal. The influence of nano-silane modifications has been covered in detail by several publications (e.g., [2,7,13]). The main advantages of nano-silane modifications of a binder include that it:

- acts effectively as an aggregate adhesive that permanently binds the bitumen to the aggregate;
- chemically alters the surface of the aggregate to become hydrophobic and repels the water from the mix; and
- assists in the stability and better distribution of the bitumen particles, effectively reducing the percentage of binder required to achieve the same engineering properties in terms of tensile and compressive strengths.

It follows that the Cape seal (20 mm stone with hand-mixed and hand-placed slurry) was constructed using a combination of previously untested binders (SASOBIT-M<sup>®</sup> tack and an anionic NME binder for the slurry with no cement or lime filler). This seal is representative of a thin asphaltic layer, with the chips held firmly in place by the slurry mix. The deformation characteristics of this thin surfacing were considered of particular interest in terms of their comparison with those of an asphalt surfacing [15]. APT on the Cape seal was included as a good indication of possible punching of the large stone size into the anionic NME-stabilised base layer, which could result in an associated over-exposure of the slurry with severe bleeding of the bitumen binder visible on the surfacing.

### 3.3. Seal Construction

The placement of the SASOBIT-M<sup>®</sup> tack coat for the 20 mm chips (stone) was done on 25 July 2018, as shown in Figure 4. With the consideration of possible future labour-intensive construction, the slurry part of the Cape seal (Section B in Figure 2) was mixed on-site using a standard concrete mixer and applied to the surfacing by hand in one application, using squeegees (Figure 5a,b). To achieve a working window of 6 h to allow the workers enough time to properly fill all voids and to achieve a smooth surface, the normal anionic NME binder was diluted with water at a 1:2 ratio during mixing with the aggregate. The required dilution of the binder resulted in an equivalent reduction in the required binder content (similar to that found with anionic stabilisation of naturally available materials where the better distribution of the binder through a reduction in particle sizes required less of the stabilising agent to meet the engineering requirements with ease).

No traffic was allowed onto the experimental section constructed as a bypass on the shoulder of an existing road before testing. This allowed for the full evaluation of the different chip and Cape seal surfacings to be done through APT loading and accurate 3D scanning without the testing and evaluation of the early-life performance being influenced by pre-loading.



Figure 4. Placement of the SASOBIT-M<sup>®</sup> tack coat for the 20 mm chips (stone).



(a)

(b)

Figure 5. On-site mixing (a) and placement (b) of the anionic NME-modified slurry mix.

#### 4. Test Equipment and Protocols

##### 4.1. Novel Use of APT Equipment

APT loading of the different chip seal sections was done using the Model Mobile Load Simulator—3rd model (MMLS3) [14]. The MMLS3 was specifically developed to test the deformation characteristics of asphalt surfacings for use on highways, with the test procedure and criteria contained in a formal South African National Standard (SANS) [15] specification. The tyre pressures of the MMLS3 are equivalent to those of heavy vehicles commonly found on southern African roads (690 kPa to 850 kPa), and loads are applied on the 300-mm-diameter tyre at 2.9 kN at a rate of 7200 repetitions per hour [14].

In this case, the standard test (100,000 repetitions at a controlled surface temperature of 50 °C) was only applied to the Cape seal containing various novel modifications in terms of the tack coat and the slurry mix. In addition, the MMLS3 was used on the three thin surfacings, applying 18,000 repetitions (high load, high frequency, high impact) to each of the test sections to evaluate the early-life performance of the thin chip seal surfacings on the base layer constructed with naturally available materials stabilised with an anionic NME stabilising agent. As discussed, the material used in the construction of the base layer is classified as unsuitable for use, even on low-volume roads. The typical setup of the MMLS3 on-site, with a graphical description of the working thereof, is shown in Figure 6.

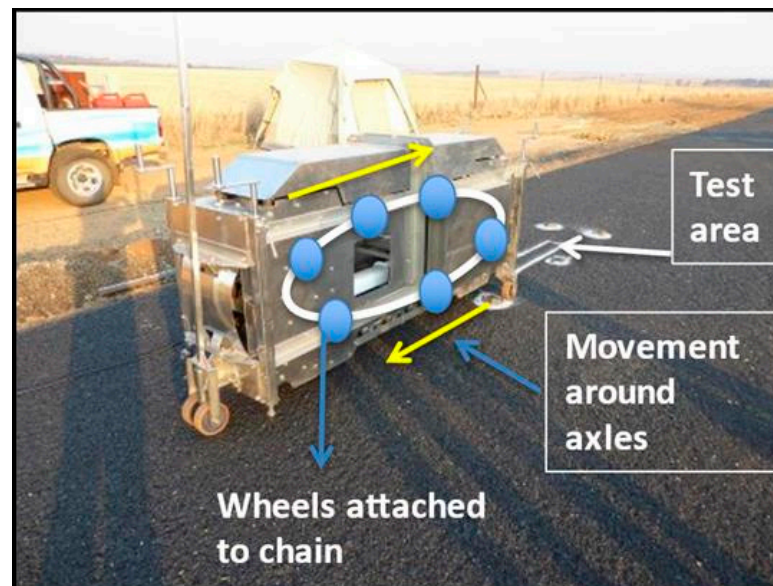


**Figure 6.** Graphical illustration of the setup and working of the 3rd Model Mobile Load Simulator (MMLS3) on-site.

#### 4.2. 3D Scanning to Determine Seal Surface Characteristics

The surface characteristics of the different seals before and after APT were determined and compared using 3D scanning with handheld EinScan equipment [16,35]. After scanning each of the samples using the handheld EinScan Pro, the digitised mesh was stored in stereolithography (STL) file format. CloudCompare (an open-source point-cloud processing tool) was used for point-cloud generation and statistical analysis. This approach provides high-accuracy assessment of the characteristics of the surfacing subjected to APT loading, allowing for an accurate statistical comparison to the surfacing without APT loading.

Due to optical limitations, the EinScan Pro is best suited for scanning lightly coloured, opaque materials. Hence, a thin layer of evenly distributed white spray paint was applied to the area to be scanned. The spray paint was applied at an angle of 45° relative to the horizon, from all cardinal directions, to ensure that the crevices and cracks were coated adequately. The minimum suitable sample size for accurate scanning was determined as 100 × 100 mm<sup>2</sup>. This sample size mitigates the effects of small, hollow voids caused by the reflective tracking markers, etc. Calibration prior to scanning was conducted, with the reported calibration accuracy shown to be within a range of 10–15 µm.

For larger aggregate sizes (>10 mm), handheld scanning provides superior angles to cover a larger percentage of the exposed surface area compared to that of a fixed scanning method. A wider range of rotation of the scanner is required to cover all areas and angles. For the Handheld HD Scan setting, an accuracy of 0.1 mm and a point distance of 0.2 to 2.0 mm is obtainable. For adequate coverage, approximately 16 scans were required around the circumference of the sample, with 2 to 3 different pitch angles for 32 to 48 scans. Typically, a point cloud composed of more than 5 million points was found to be indicative

of a complete scan. The scanning process takes approximately 20 min per sample. The scans are scaled in the appropriate unit of measurement (millimetres). For samples selected at random locations, the surface area varied by less than 2%.

Analysis of the digitised samples was performed using CloudCompare. Distributions of roughness, curvature and point densities were performed and compared for different samples and specimens with the built-in functionality. Considering the resolution of the scanner and the sample size, a point-cloud density of 100 points/mm<sup>2</sup> was found to have sufficient resolution and repeatability. This equates to 1,000,000 points for a 100 mm × 100 mm sample. A typical example of an imported mesh of the 20 mm stone prior to APT loading is shown in Figure 7.

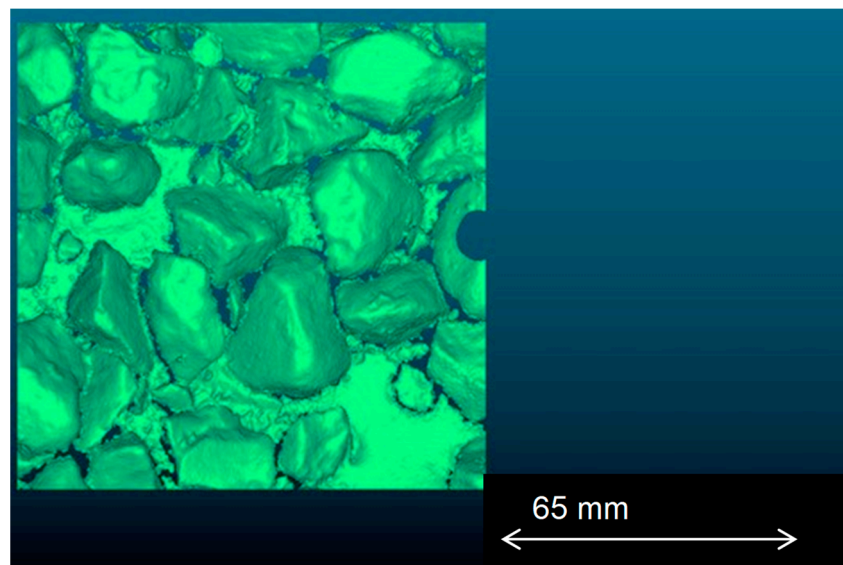


**Figure 7.** Typical example of an imported mesh of the 20 mm single seal.

#### 4.3. Characterisation of the Chip Seal Surface Characteristics

The Mean Profile Depth (MPD) and Mean Texture Depth (MTD) calculations were done using the data obtained from the handheld 3D scanning equipment. The surface characteristics of the different seals before and after APT loading were determined and compared using the 3D scans. The MPD is calculated as the average profile depth of two sections (using the highest peak on each section) over a 100-mm-long baseline [36].

The sand patch test [37] uses a volumetric approach of measuring pavement macrotexture. The MTD [15] can be expressed as the ratio of the volume of material that is required to fill the surface, divided by the area that is covered by the volume of material. Unlike the American Society for Testing Materials (ASTM) method, the surface area of the sample remains fixed when using 3D scanning technology, with the volume of the material filling the surface texture serving as the variable quantity. The benefit of this calculation is that an equivalent sand patch value can be calculated directly using the software. The volume of both the cuboid surrounding the sample (area multiplied by the greatest difference in height) and the volume of the aggregate are known. The difference in the volume is occupied by the virtual sand particles that would fill the surface until the entire surface is covered uniformly.

Two quantitative metrics were used for describing the relevant surfacing characteristics. For each sample, the kernel size was configured to be between 25% and 100% of the nominal aggregate dimension. Smaller kernel sizes provided improved representative statistics of the samples. The two metrics that were found to provide good results are curvature and roughness.

The built-in curvature tool provides an assessment of the extrinsic mean curvature that is derived from a differential geometry. The curvature of each point is estimated by

best fitting a quadratic around that particular point. A histogram provides the distribution of the metric. The roughness distribution is based on a best-fitting plane of the surrounding points within the kernel. The roughness will thus be highly dependent on the volume and shape of the aggregate protruding from the seal or binder surface. The statistical data can be expressed using either a Weibull distribution with a- and b-parameters describing the scale and shape, respectively, or an exponential distribution. The goodness-of-fit is highly dependent on the aggregate dimensions and shape for each test.

## 5. APT Loading and Evaluation of the 3 Different Seals Using the MMLS3

### 5.1. Comparing the 3D Scans of the Three Different Thin Surfacing Subjected to APT Loading with Adjacent Areas Subjected to No Loading

#### 5.1.1. General

The two-chip seal and the Cape seal APT sections were evaluated using the 3D scanning technology and statistical evaluation tools described. The main objectives of these tests were to evaluate the performance of thin, cost-effective surfacings on an anionic NME-stabilised base using naturally available materials. Simultaneously, the opportunity was used to test the use of unconventional binders that would provide contractors with more leniency with regard to the strict specifications applicable to the successful placement of chip seals at a lower risk.

#### 5.1.2. Single 20 mm Chip Seal with 1.5% SASOBIT-M<sup>®</sup>-Modified 60/70 Pen Bitumen

Visual assessment: The demarcated area for the APT loading done on the 20 mm single seal with the area for the 3D scans painted in white is shown in Figure 8. The stone reorientation that occurred on the 20 mm single seal after 18,000 repetitions is clearly visible. No stone loss could visibly be detected on the test section, and no stone penetration into the anionic NME-stabilised base (using unsuitable materials) could be detected.



**Figure 8.** Condition of the 20 mm single chip seal in and outside the APT area.

A 3D scan of the surfacing with and without loading: The height maps of the 20 mm seal produced from the 3D scans are shown in Figure 9 (APT loading on the left and no loading on the right). The blue-to-red 3D-generated pictures show the relative differences in height within the scanned areas. The less red in the scan after APT loading is an indication of the reorientation of the stone that has taken place and the filling of the vacant blue areas. The statistical evaluations of the data of the two scanned areas are given in Table 2.

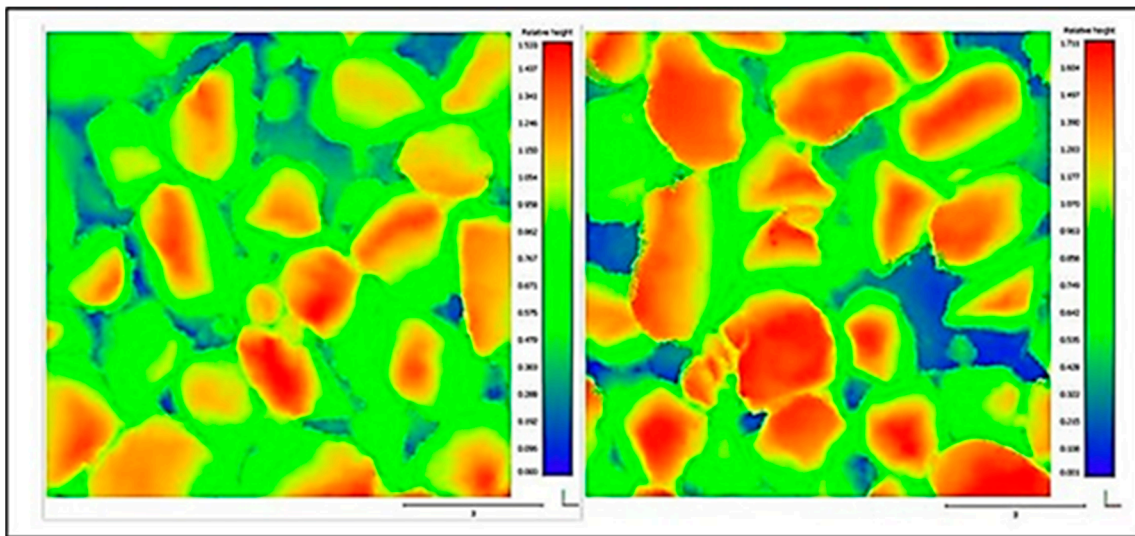


**Figure 9.** A 3D scan of the 20 mm single seal. Left: APT loading. Right: no loading.

**Table 2.** Volume and void ratios calculated from a statistical analysis of the 3D scans of the single 20 mm seal shown in Figure 9.

Parameter	APT Loading	No Loading
Solid volume ( $V_T$ ) ( $\text{cm}^3$ )	156.22	178.88
Sample area ( $\text{cm}^2$ )	100.2	100.2
Largest height difference (mm)	15.6	17.9
Aggregate volume ( $V_s$ ) ( $\text{cm}^3$ )	84.83	110.40
Void volume ( $V_v$ ) ( $\text{cm}^3$ )	71.39	68.48
Void ratio ( $V_v/V_s$ )	0.84	0.62
Void ratio ( $V_v/V_T$ )	0.46	0.38
Mean texture depth (MTD) (mm)	7.14	6.85
Mean profile depth (MPD) (mm)	6.34	5.76

### 5.1.3. A 20/7 mm Double Seal with a SASOBIT-M<sup>®</sup> Tack Coat and an Elastomer-(SBS)-Modified (S-E2) Second Application Followed by a Fog Spray

Visual assessment: Figure 10 shows the surfacing of the double seal with and without testing with more than 18,000 repetitions applied at temperatures between 12 °C and 19 °C with the MMLS3. No visible difference between the test area and untested surfacing was detected. No sign of an excess of binder could be detected on any of the test sections, with no sign of bleeding of the binder.

A 3D scan of the double chip seal surfacing with and without loading: The 3D scan images generated on the double seal are shown in Figure 11. Although a visual difference could not be detected by eye, the 3D scan images show a clear difference between the surfaces with and without loading. The height maps generated from the image are shown in Figure 12. The areas subjected to APT loading (left in Figures 11 and 12) clearly show a denser matrix when compared to the adjacent area where no loading was applied (right in Figures 11 and 12). It follows that the smaller 7 mm stone was packed closer into the first 20 mm seal under loading, leaving fewer gaps and moving towards a more densely packed, uniform surface. The volume and void ratios calculated from the scan data sets are given in Table 3.



Figure 10. Condition of the 20/7 double seal after APT at <math><20\text{ }^\circ\text{C}</math>.

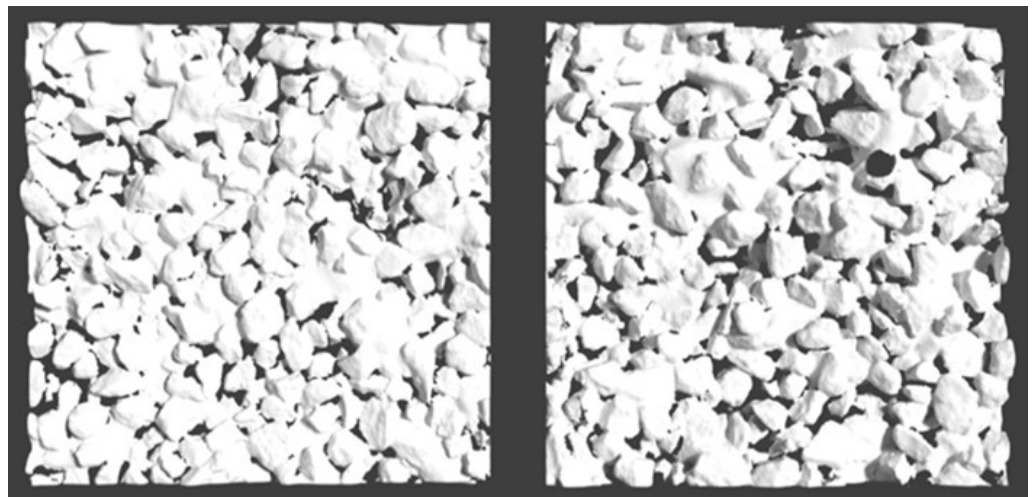


Figure 11. A 3D scan image of the area subjected to APT loading (left) and the adjacent area (right) that received no loading.

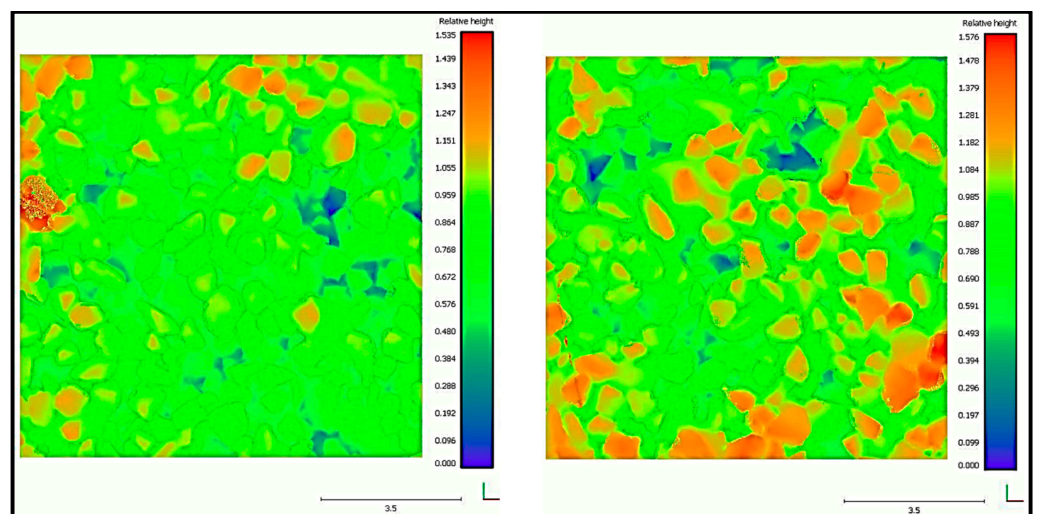


Figure 12. Height maps obtained from the 3D scans of the area subjected to APT loading (left) and the adjacent section (right) that received no loading.

**Table 3.** Volume and void ratios calculated from a statistical analysis of the 3D data sets on the double seal shown in Figures 11 and 12.

Parameter	APT Loading	No Loading
Solid volume ( $V_T$ ) ( $\text{cm}^3$ )	81.50	93.16
Sample area ( $\text{cm}^2$ )	100.2	100.2
Largest height difference (mm)	15.4	15.8
Aggregate volume ( $V_S$ ) ( $\text{cm}^3$ )	21.67	28.01
Void volume ( $V_V$ ) ( $\text{cm}^3$ )	59.84	65.25
Void ratio ( $V_V/V_S$ )	2.76	2.33
Void ratio ( $V_V/V_T$ )	0.73	0.67
MTD (mm)	5.97	6.50
MPD (mm)	3.81	3.57

The area subjected to APT loading (left in Figure 12) illustrates the reorientation of the chips with less protruding features above the surface. The distribution of curvature shifts correspondingly towards lower values, i.e., uniformity. The roughness distribution indicates roughness values between 0.6 mm and 1.0 mm that is likely a representation of the surface roughness of the aggregates rather than macroscopic dimensions.

5.1.4. A 20 mm Cape Seal with 1.5% SASOBIT-M<sup>®</sup>-Modified Tack Coat and an Anionic Nano-Silane-Modified Bitumen Emulsion Slurry without Any Cement/Lime Filler—First Test: 18,000 Repetitions Applied with the MMLS3 at Temperatures between 12 °C and 19 °C

Visual assessment: Figure 13 shows the surfacings of the Cape seal subjected to loading. A slightly rougher surface could be detected in the test area, indicating that the 20 mm stone did not penetrate into the base but that the slurry actually filled any voids that was not properly filled during the placement of the slurry by hand.



**Figure 13.** Condition of the Cape seal after APT at <20 °C.

A 3D scan of the surfacing with and without loading: The height maps of the 20 mm Cape seal produced from the 3D scans are shown in Figure 14. The statistical evaluations of the data of the two data sets are given in Table 4. The 3D scans and the statistical analyses of the data confirm the visual observations.

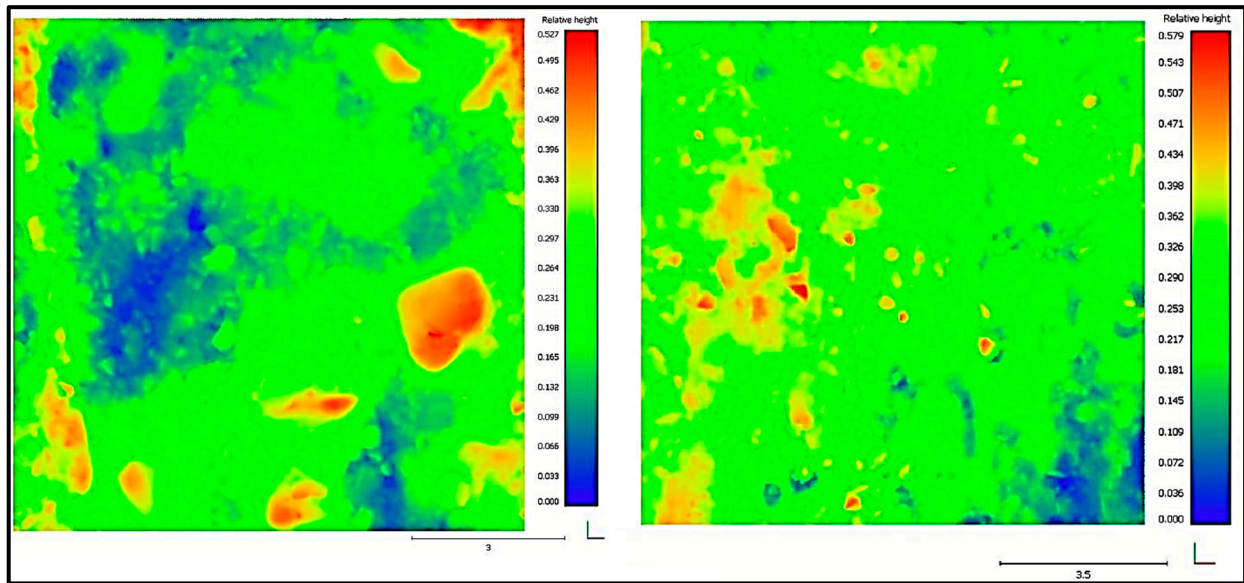


**Figure 14.** A 3D scan of the 20 mm Cape seal. Left: APT loading. Right: no loading.

**Table 4.** Volume and void ratios calculated from a statistical analysis of 3D scans of the Cape seal.

Parameter	APT Loading	No Loading
Solid volume ( $V_T$ ) ( $\text{cm}^3$ )	52.81	58.92
Sample area ( $\text{cm}^2$ )	100.2	100.2
Largest height difference (mm)	5.3	5.9
Aggregate volume ( $V_S$ ) ( $\text{cm}^3$ )	21.67	28.01
Void volume ( $V_V$ ) ( $\text{cm}^3$ )	31.14	30.91
Void ratio ( $V_V/V_S$ )	1.44	1.10
Void ratio ( $V_V/V_T$ )	0.59	0.53
MTD (mm)	3.11	3.08
MPD (mm)	1.83	1.59

The APT loading sample (left) illustrates more pronounced visibility of the 20 mm aggregate from below the slurry mix. This is likely due to the reorientation of the smaller particle sizes in the slurry mix moving towards a more closely packed, stable state. From the roughness analysis, it is seen that the APT area (left) illustrates the exposure (appearance) of the larger 20 mm aggregate. This could be an indication that not all voids were filled during the hand placement of the slurry mix.

#### 5.1.5. A 20 mm Cape Seal—Second Test: Full APT Loading—Standard 100,000 Repetitions Applied within 24 h with the MMLS3 at a Controlled Temperature of 50 °C

Visual and measured assessment: The comparative surfacings of the full 24 h MMLS3 test with 100,000 repetitions at 50 °C are shown in Figure 15, with the test area enhanced to emphasize the differences in visual appearance.

The deformation measurements taken at different point along the test section, at different load repetitions of the full standard APT using the MMLS3 [15], on the Cape seal, are given in Table 5. The averages of the profile measurements as a function of the load results are shown in Figure 16. The average rut versus load repetitions and the extrapolation of the result to a million repetitions are shown in Figure 17.

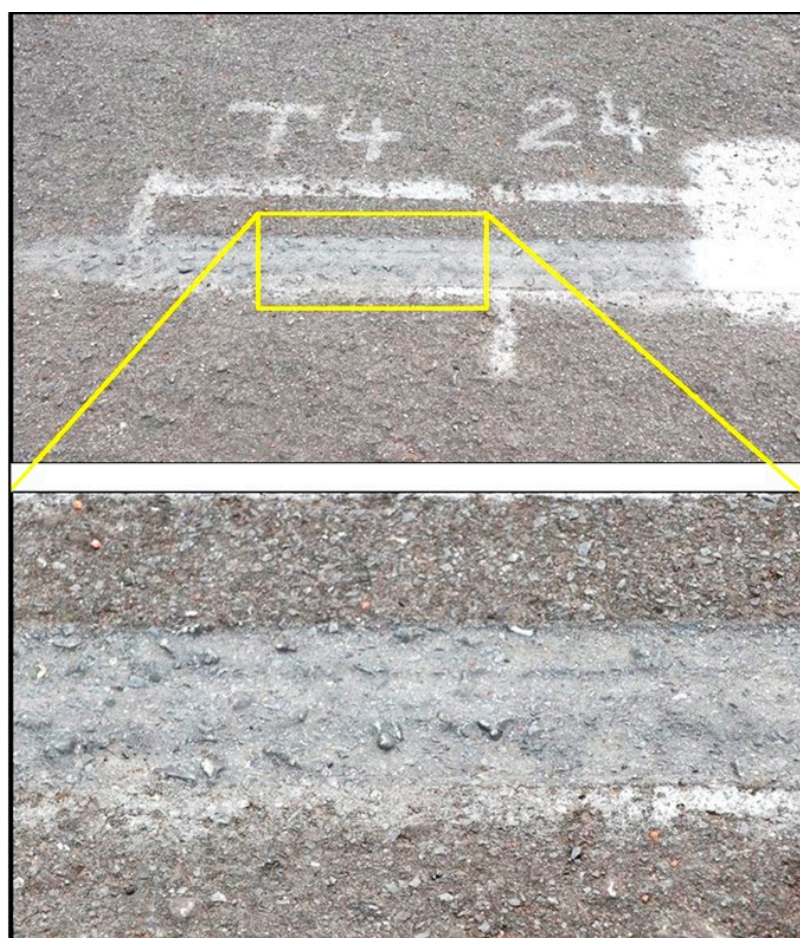


**Figure 15.** Condition of the Cape seal after a full-scale 24 h MMLS3 (APT) test at 50 °C applying 100,000 load repetitions.

**Table 5.** Summary of the rut depth measurements at various positions and repetitions of the standard MMLS3 test (South African National Standard (SANS) 3001-DP1) [15], done on the Cape seal with an anionic NME slurry mix placed on an anionic NME-stabilised base constructed with naturally available materials (Table 1—materials quality G8/A-2-6).

Measured Rut (mm) at Different Axle Load Repetitions at Different Positions in the Test Areas							
Position	0	2500	5000	10,000	25,000	50,000	100,000
0100	0	1.69	2.05	2.38	2.57	2.84	3.03
0200	0	1.86	2.04	2.34	2.56	2.83	2.98
0300	0	3.04	3.24	3.54	3.87	4.10	4.22
0400	0	2.80	3.06	3.40	3.99	4.35	4.69
0500	0	2.63	2.91	3.29	3.60	3.90	4.13
0600	0	2.56	2.65	2.86	3.15	3.37	3.82
0700	0	2.56	2.65	2.86	3.15	3.37	3.62
0800	0	2.94	3.03	3.42	3.71	4.05	4.25
0900	0	2.59	2.67	2.86	3.00	3.13	3.46
Mean (Average)	0	2.58	2.76	3.07	3.38	3.65	3.87
Std. dev.	0.00	0.50	0.45	0.48	0.57	0.61	0.63
COV * %	0	19.4	16.3	15.6	16.9	16.7	16.3

Average rutting @ 100,000 repetitions = 3.87 mm

\* COV % = Coefficient of Variation % = (Standard Deviation/Mean) × 100

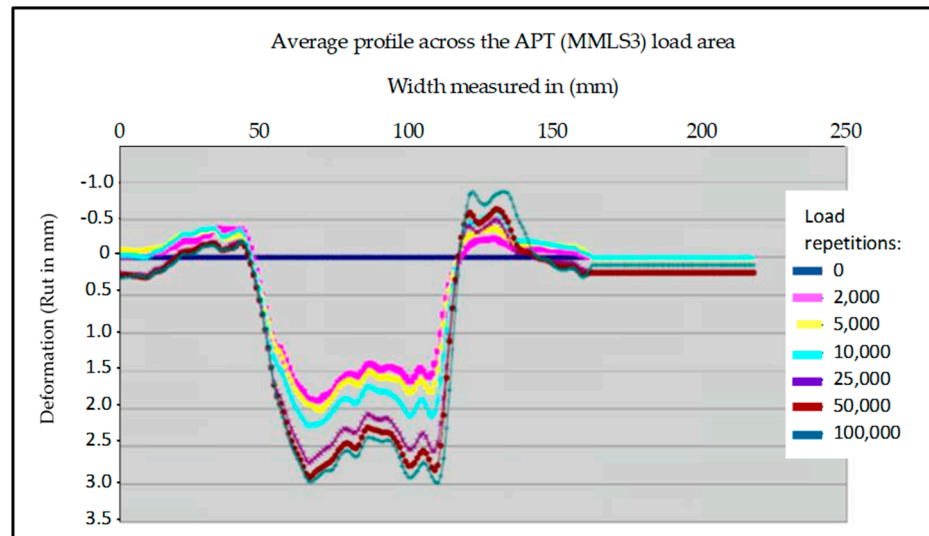


**Figure 16.** Average of the profile measurements taken at various repetitions during the full MMLS3 test (APT) done on the Cape seal.

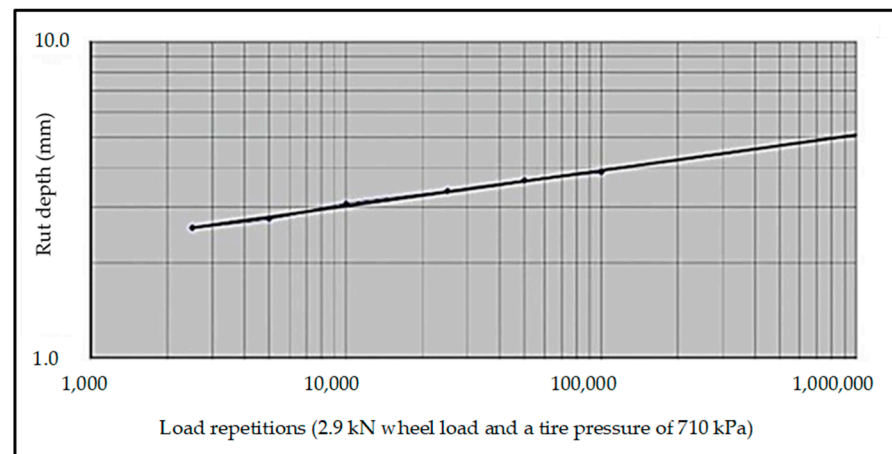


**Figure 17.** Plot and extrapolation of the average measured rut depth during the 24 h MMLS3 test with 100,000 repetitions done on the Cape seal constructed using unconventional binders.

A test result of a rut depth measurement of less than 3 mm is considered adequate for the future expected deformation behaviour over the design period of the asphalt surfacing on highways [14,15]. The measured rut depth on the Cape seal after the test was less than 4 mm. Considering the test results in the context of the design traffic loading (1 million E80s) and the material used, the rut depth performance of the Cape seal with the novel modified binders on the base layer consisting of materials classified as unsuitable, stabilised with an anionic NME stabilising agent, can be considered as more than satisfactory.

A 3D scan of the surfacing with and without loading: The height maps generated from the 3D scans are shown in Figure 18. The volume and void ratios calculated from the data sets are shown in Table 6. Similar to the previous MMLS3 test with only 18,000 repetitions at a temperature of less than 20 °C, the area subjected to APT loading (left) again shows protruding of the 20 mm aggregate from between the slurry. This result confirms the conclusion that not all voids were filled during the application of the slurry mix and there was no punching of the stone into the anionic stabilised base layer. Both the MTD and the MPD increased during APT loading.

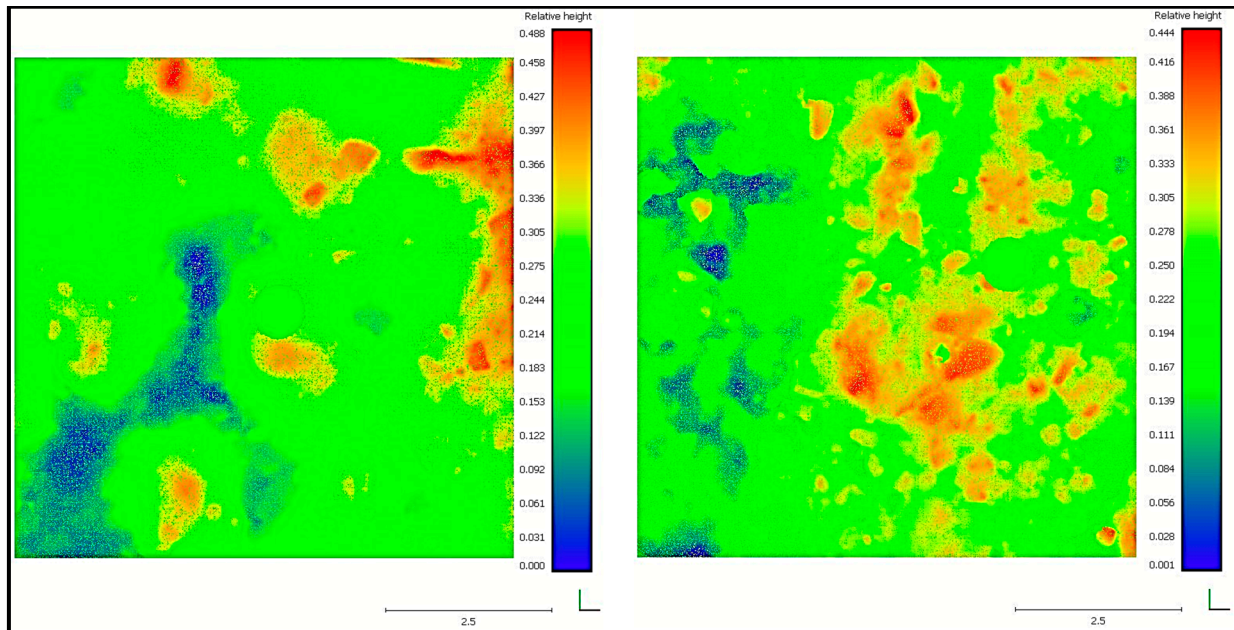


**Figure 18.** Height maps generated from the 3D scan of the area subjected to standard APT loading in order to assess the rut of the Cape seal.

**Table 6.** Volume and void ratios calculated from a statistical analysis of the 3D data sets of the 24 h test done on the Cape seal.

Parameter	APT Loading	No Loading
Solid volume ( $V_T$ ) ( $\text{cm}^3$ )	27.523	24.985
Sample area ( $\text{cm}^2$ )	56.4	56.4
Largest height difference (mm)	4.88	4.48
Aggregate volume ( $V_S$ ) ( $\text{cm}^3$ )	13.305	13.619
Void volume ( $V_V$ ) ( $\text{cm}^3$ )	14.218	11.366
Void ratio ( $V_V/V_S$ )	1.069	0.835
Void ratio ( $V_V/V_T$ )	0.517	0.455
MTD (mm)	2.52	2.02
MPD (mm)	1.43	1.40

### 5.2. Visual Inspection: 19 March 2020

The test section was again visually inspected on 19 March 2020. No traffic has used the test section for 14 months since January 2019. The single seal and the Cape seal (Figure 19) showed no difference. However, closely spaced (about 100 mm apart) small holes were now clearly visible all over the double seal section (Figure 20). These holes showed excess binder visible on top of the surfacing, indicating the forceful escape from the bottom of trapped moisture vapor that popped through the second application of the modified (S-E2) [11] elastomer-(SBS)-modified binder. The size of the holes can be compared to the lens cap of a camera, partially shown in Figure 20. The different novel binder applications used in the Cape seal and the single seal showed no holes, with no visible sign of moisture entrapment.

The tack coat on all the chip seal sections is the same, i.e., a SASOBIT-M<sup>®</sup>-modified binder. The only difference in binder application that could lead to this observed performance on the double seal is in the binders used in applying the second layer (7 mm) of the double chip seal and the anionic NME-modified binder used in the slurry mix. The second application on the double seal and the binder used in the slurry mix are the only differences in binder application between the two sections. It is logically concluded that the modified binder used on the second seal of the double seal—an elastomer modified SBS binder (S-E2) [11]—did not allow for the evaporation of moisture from the anionic

NME base to continue, confirming a disadvantage that is clearly noted in the Technical Guidelines (TG1) [11] document.



**Figure 19.** March 2020—condition of the Cape seal.



**Figure 20.** March 2020—condition of the double seal showing multiple holes all over the test section with excess binder on the top of the surfacing surrounding the holes.

## 6. Summary of the Discussion of Results

The test results confirmed that the application of the chips (aggregate) of a chip seal using a SASOBIT-M<sup>®</sup>-modified binder at temperatures considerably lower than current recommendations can be done at low risk. In addition, reorientation of the stone took place under APT loading applied at temperatures less than 20 °C (12 °C to 19 °C) without any apparent stone loss. These observations were confirmed both visually and using 3D scans of the surfacings on the 20 mm single chip seal areas. The tack coat on all the various test sections was applied at a road surface temperature of approximately 18 °C, i.e., 7 °C less than the minimum recommended best practice of 25 °C and rising [15], with no apparent stone loss. No punching of the chips (stone) into the newly constructed anionic NME-stabilised base layer could be observed (constructed with naturally available materials classified as unsuitable for use in the base and sub-base layers of a pavement structure).

The initial APT loading areas with the high-load, high-frequency MMLS3 showed no visually detectable differences between the areas subjected to APT loading and the adjacent areas on the double seal and very little difference on the Cape seal test sections. However, the 3D scans clearly indicated that reorientation of the stone occurred on both the Cape seal (protrusion of the bigger 20 mm stone) and the double seal (closer matrix due to compaction under loading and stone reorientation). No stone loss could be detected on any of the three experimental surfacing sections subjected to APT loading at temperatures below 20 °C. No visible or measured punching of the stone into the anionic NME-stabilised base layer could be detected.

The 3D scans done to compare areas subjected to loading with the adjacent areas gave an objective and quantitatively measurement of the effect of the load applications through the generated 3D surface maps and the statistical analyses of the data sets. Much of these differences could not be detected visually. The resulting point clouds from the 3D scans also made it visually obvious what happened with regard to stone reorientation and change in surface characteristics under the effect of APT loading.

The full-scale APT on the Cape seal gave remarkably good results (less than 4 mm deformation), especially considering the thickness of the surfacing and the quality of the materials used in the base layer. The protrusion of the larger 20 mm stone was also more pronounced compared to the scans done during the initial 18,000 repetition test (MPD and MTD data in Tables 4 and 6). The MPD and MTD data from all the test sections are summarised in Figures 21 and 22. These results could detect no evidence of the punching of the 20 mm stone into the top of the base layer—even after the standard 100,000-repetition test done at a controlled temperature of 50 °C. The anionic NME stabilisation of the materials used in the base layer enabled the material to develop the required engineering strengths to withstand the APT loading and perform considerably better than indicated by the traditional material classification system.

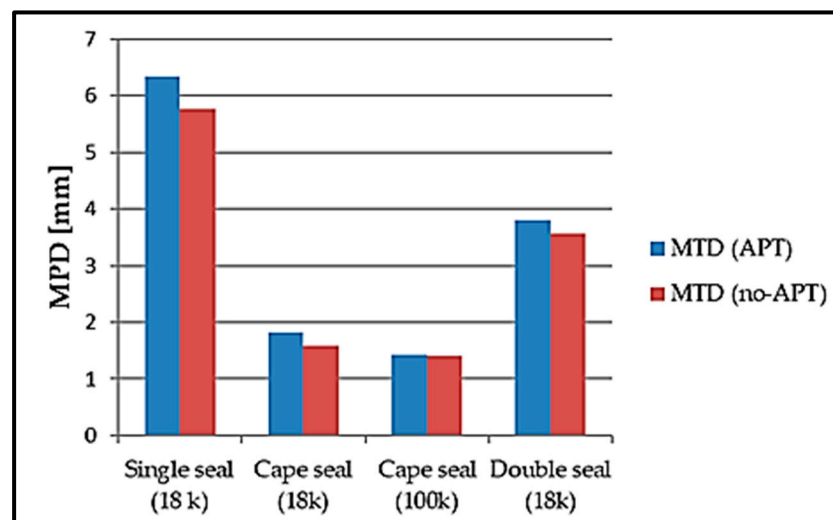


**Figure 21.** Comparative Mean Profile Depth (MPD) between the various chip seal surfacings both with and without APT loading.

The visual inspection done 14 months after the last traffic on the test sections was significant in terms of findings regarding binder selection on newly constructed layers where evaporation of moisture is expected to continue. The formation of numerous holes on the double seal clearly shows that the applicability of a binder that allows for the evaporation of moisture to continue is an important criterion to be considered when binders are specified. Under normal traffic conditions, the continuous wheel loadings would most probably have sealed those holes in the wheel tracks, preventing the escape of moisture within the wheel-tracks. With the base material having been modified to repel

water, the entrapment of the moisture vapor could result in the stripping of the surfacing or movement of the moisture to areas outside the wheel-tracks to escape, resulting in excess binder and bleeding on the wheel-track edges. In both scenarios the entrapment of the moisture vapour could result in early-life distress within the first year after opening to traffic.

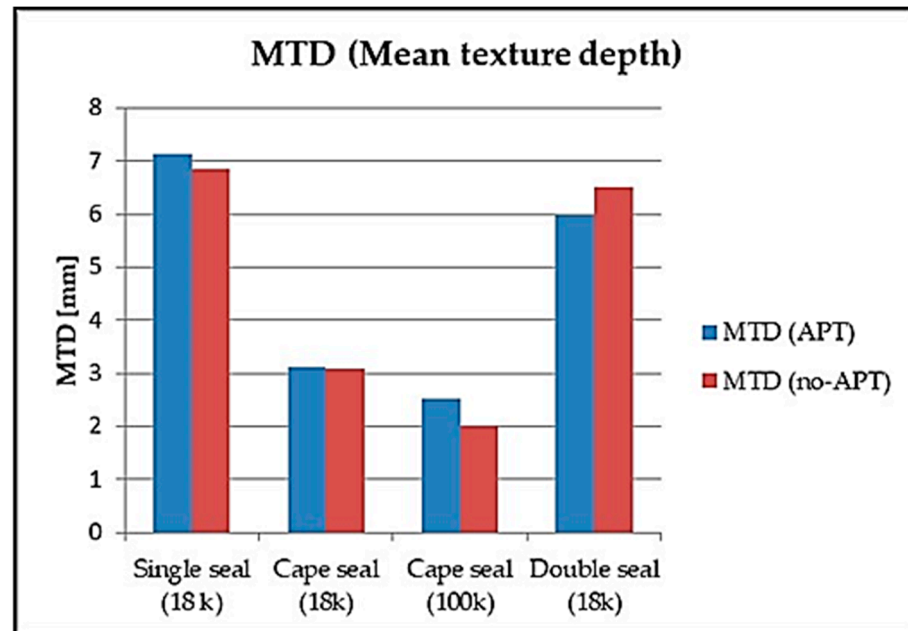


**Figure 22.** Comparative Mean Texture Depth (MTD) between the various chip seal surfacings both with and without APT loading.

## 7. Conclusions and Recommendations

The cost-effective combination of thin chip and Cape seal surfacings for use on a highly flexible pavement containing a base layer consisting of sub-standard naturally available materials stabilised with a material compatible anionic New-age (nano)-Modified Emulsion (NME) was successfully tested and accurately quantified and evaluated using APT equipment and 3D scanning technologies. The design of the thin chip and Cape seal surfacings was done to specifically evaluate possible early-life failure at the top of the base layer with punching of the stone into the newly stabilised base layer.

In addition, the three test sections were designed with novel modified binders to address risks associated with the construction of chip and Cape seals. These risks are specifically associated with the minimum binder temperatures required to minimise stone loss as well as early-life failures under loading (during the orientation of the stone) at temperatures below 20 °C (also associated with stone loss and seal failures).

The APT MMLS3 equipment used was originally designed to evaluate the deformation (rut potential) of asphalt surfacings for highways. On these test sections, it was used to evaluate the early-life performance of the different surfacing seals during critical temperature conditions as well as possible penetration of the stone (chips) from the surfacing into the base layer. Evaluation of the results was done visually and analysed using 3D hand-scanning technology to generate 3D point clouds from which accurate statistical models of the surfacings with and without APT loading could be generated. Hence, surfacing characteristics could be determined with a high degree of accuracy and repeatability.

A SASOBIT-M<sup>®</sup> tack coat with a 20 mm seal was successfully applied over the whole test area at a road surface temperature of 18 °C (7 °C less than the recommended minimum of 25 °C) with no visible stone loss. In addition, in a single chip seal section, part of a 20 mm chip seal was turned into a Cape seal using a slurry mix done with an anionic NME binder with no cement or lime filler. The slurry mix was prepared next to the road and

placed by hand. A third test section was done where the 20 mm first chip seal was turned into a double chip seal with an elastomer (SBS)-modified binder using a 7 mm stone size.

All three test sections were tested with the MMLS3 at temperatures between 12 °C and 19 °C with no apparent stone loss and no penetration of the stone into the newly constructed NME-stabilised base layer. The selection of the specific modified binders proved successful to reduce construction risks normally associated with chip seal surfacings. The anionic NME-stabilised base constructed using sub-standard materials developed early strengths required to prevent stone penetration into the top of the base. This type of distress often results in associated bleeding of the binder and failure at the top of the base layer with normal bitumen emulsion stabilisation of materials of acceptable quality (in terms of traditional classification systems). All results were confirmed using the handheld 3D scanner and the accurate statistical analysis of the 3D point clouds developed with the scans of all APT sections.

In addition to the initial testing done at temperatures below 20 °C, the Cape seal section was also subjected to a standard 24 h, 100,000-repetition MMLS3 test at a controlled temperature of 50 °C. This test was designed for the evaluation of asphalt layers on highways, specifying a maximum rut deformation of 3 mm at the end of the test [15], using the standard MMLS3 APT apparatus. The maximum deformation measured on the Cape seal was less than 4 mm, a remarkable result considering the thickness of the surfacing, the quality of the materials used in the NME-stabilised base layer and a design traffic loading of only 1 million standard 80 kN dual-wheel axle loads (E80s). The anionic NME stabilisation enabled the material in the base layer to perform considerably better than indicated by the traditional material classification system.

The visual inspection done on the test areas after 14 months of no trafficking showed multiple small, clearly visible holes over the whole of the double seal section. No such problems were observed on the single seal or the Cape seal sections. The use of an elastomer modification of the binder on the second seal, which is known to “restrict evaporation of entrapped moisture”, is the only difference in terms of binder usage compared to the other surfacings. To escape, the evaporated moisture forced (popped) through the binder, leaving excess binder on the top of the surfacing with a resultant hole in the surfacing. It follows that limitations with regard to the breathability in the selection of an applicable modified binder for use on any newly constructed base layer is an important factor, requiring careful consideration.

All three thin surfacings were also subjected to normal traffic loading during a heat-wave in December 2018 with no visible signs of bleeding. The application of the tack coat with a binder modified with 1.5% SASOBIT-M<sup>®</sup> applied with a 20 mm first chip seal tested under abnormal temperature conditions is considered to be a success, warranting further investigation in terms of limits of application. This modified binder may well reduce the risk of failure associated with construction limitations.

It has been shown that the stabilisation of naturally available materials for use in base layers can successfully be combined with thin chip or Cape seal surfacings, without an increase in the risk of early-life failure. Considering the relatively poor quality of material used in the construction of the NME-stabilised base, a considerable margin of error was built into these test sections. The positive results obtained from the tests done using these novel binder modifications with thin chip and Cape seal surfacings warrant further investigation in terms of possible inclusion in future specifications.

**Author Contributions:** G.J.J. under the directive of the head of the Department of Civil Engineering, W.J.v.M.S., has been leading the research into the provision of affordable road infrastructure at the Faculty of Engineering, University of Pretoria. W.J.v.M.S. recognised the potential of a nanotechnology solution in the field of pavement engineering more than a decade ago. G.J.J. through involvement in the private sector and the support of road authorities, has been instrumental in the development of a scientific principle, ensuring that implementation can be achieved at minimum risk. The PhD candidate A.B. has been instrumental in the implementation, measurement and analysis of the 3D scanning done on the various surfacings and doing the comparisons of the various test sections

with and without APT loading. All authors have read and agreed to the published version of the manuscript.

**Funding:** This research received no external funding.

**Institutional Review Board Statement:** Not applicable.

**Informed Consent Statement:** Not applicable.

**Data Availability Statement:** Not applicable.

**Acknowledgments:** The support of GeoNANO Technologies (Pty) Ltd., 18 Davies road, Wychwood, Germiston, 1401, South Africa (Tel.: +27-844078489; [www.geonano.co.za](http://www.geonano.co.za) (accessed on 26 January 2021), [info@geonano.co.za](mailto:info@geonano.co.za)) for students at the Department of Civil Engineering, University of Pretoria, Pretoria, South Africa, to test a wide variety of materials as part of final-year projects and post-graduate theses, testing the various principles identified in this paper, is acknowledged. SASOL SA is acknowledged for its assistance in the application of the SASOBIT-M© binder and the APT thereof. XRD Analytical and Consulting cc, Pretoria, is acknowledged for assisting students with the X-ray Diffraction (XRD) analysis of material samples. Roadlab Civil Engineering Materials Testing Laboratory, Germiston, 1401, South Africa, is acknowledged for assistance to students with basic material indicator testing.

**Conflicts of Interest:** The authors declare no conflict of interest.

## References

1. Southern Africa Transport and Communications Commission (SATCC). *Guideline: Low-Volume Sealed Roads*; Southern Africa Development Community (SADC), SADC House: Gaborone, Botswana, 2003; ISBN 99912-0-456-5.
2. Jordaan, G.J.; Kilian, A. The Cost-effective Upgrading, Preservation and Rehabilitation of Roads—Optimising the Use of Available Technologies. In Proceedings of the Southern African Transport Convention (SATC 2016), CSIR, Pretoria, South Africa, 4–7 July 2016.
3. Jordaan, G.J.; Kilian, A.; Muthivelli, N.; Dlamini, D. Practical Application of Nano-Technology in Roads in southern Africa. In Proceedings of the 8th Transportation Technology Transfer (T2) Conference, Lusaka, Zambia, 8–10 May 2017.
4. Rust, F.C.; Alkhalwaya, I.; Jordaan, G.J.; Du Plessis, L. Evaluation of a nano-silane-modified emulsion stabilised base and subbase under HVS traffic. In Proceedings of the 12th Conference on Asphalt Pavements for Southern Africa (CAPSA 2019), Sun City, South Africa, 13–16 October 2019.
5. Rust, F.; Smit, M.; Alkhalwaya, I.; Jordaan, G.; Du Plessis, L. Evaluation of two nano-silane-modified emulsion stabilised pavements using accelerated pavement testing. *Int. J. Pavement Eng.* **2020**, *1*–14. [[CrossRef](#)]
6. Jordaan, G.J.; Kilian, A.; Du Plessis, L.; Murphy, M. The development of cost-effective pavement design approaches using mineralogy tests with new nano-technology modifications of materials. In Proceedings of the Southern Africa Transportation Conference (SATC 2017), Pretoria, South Africa, 10–13 July 2017.
7. Jordaan, G.J.; Steyn, W.J. *A Comprehensive Guide to the Use of Applicable and Proven Nano-Technologies in the Field of Road Pavement Engineering Design and Construction*; Department of Civil Engineering, University of Pretoria: Pretoria, South Africa, 2019; ISBN 978-0-620-83022-5.
8. Jordaan, G.; Steyn, W. Fundamental Principles Ensuring Successful Implementation of New-Age (Nano) Modified Emulsions (NME) for the Stabilisation of Naturally Available Materials in Pavement Engineering. *Appl. Sci.* **2021**, *11*, 1745. [[CrossRef](#)]
9. Li, J.; Luhr, D.R.; Russell, M.; Rydholm, T.; Uhlmeier, J.S. Cost-Effective Performance Management for Washington State Pavement Assets. *Transp. Res. Rec. J. Transp. Res. Board* **2017**, *2639*, 102–109. [[CrossRef](#)]
10. Khattak, M.J.; Baladi, G.Y. *Development of Cost-Effective Treatment Performance and Treatment Selection Models*; Louisiana Transportation Research Board Centre: Baton Rouge, LA, USA, 2015. Available online: <http://www.ltrc.lsu.edu/pdf/2015/FR518.pdf> (accessed on 13 February 2021).
11. SABITA. *TG1: The Use of Modified Bituminous Binder in Road Construction*, 3rd ed.; Southern African Bitumen Association (SABITA): Cape Town, South Africa, 2015; ISBN 978-1-874968-67-2.
12. Porto, M.; Caputo, P.; Loise, V.; Eskandarsefat, S.; Teltayev, B.; Rossi, C.O. Bitumen and Bitumen Modification: A Review on Latest Advances. *Appl. Sci.* **2019**, *9*, 742. [[CrossRef](#)]
13. Caputo, P.; Porto, M.; Angelico, R.; Loise, V.; Calandra, P.; Rossi, C.O. Bitumen and asphalt concrete modified by nanometer-sized particles: Basic concepts, the state of the art and future perspectives of the nanoscale approach. *Adv. Colloid Interface Sci.* **2020**, *285*, 102283. [[CrossRef](#)] [[PubMed](#)]
14. Hugo, F.; Steyn, W.J.v.M. A synthesis of applications of the MLS as an innovative system for evaluating performance of asphalt materials in pavement engineering. In Proceedings of the 11th Conference on Asphalt Pavements for Southern Africa (CAPSA 2015), Sun City, South Africa, 16–19 August 2015.

15. South African National Standards (SANS). *3001-PD1:2016 ED.1 Civil Engineering Test Methods Part PD1: Determination of Permanent Deformation and Moisture Sensitivity in Asphalt Mixes with the MMLS3*; South African Bureau of Standards (SABS) Standards Division: Pretoria, South Africa, 2016.
16. Steyn, W.J.v.d.M.; Broekmam, A.; Jordaan, G.J. Digital twinning of asphalt pavement surfacings using Visual Simultaneous Localization and Mapping. In Proceedings of the 2nd International Conference on Advances in Materials and Pavement Performance Prediction (AM3P 2020), San Antonio, TX, USA, 27–29 May 2020. [[CrossRef](#)]
17. American Society for Testing Materials ASTM Standard D698. *Standard Test Methods for Laboratory Compaction Characteristics of Soil Using Standard Effort*; ASTM International: West Conshohocken, PA, USA, 2007. [[CrossRef](#)]
18. American Society for Testing Materials ASTM Standard D1557. *Standard Test Methods for Laboratory Compaction Characteristics of Soil Using Modified Effort*; ASTM International: West Conshohocken, PA, USA, 2009. [[CrossRef](#)]
19. National Transport Commission. *Technical Methods for Highways TMH1: Standard Methods of Testing Road Construction Materials*; Committee for State Road Authorities, Department of Transport: Pretoria, South Africa, 1986.
20. Committee of Land Transport Officials (COLTO). *Guidelines for Road Construction Materials*; South African Institution of Civil Engineers (SAICE): Halfway House, South Africa, 1985.
21. American Association of State and Highway Transportation Officials (AASHTO). *M145-91: Standard Specification for Classification of Soils and Soil-Aggregate Mixtures for Highway Construction Purposes*; American Association of State Highway and Transportation Officials (AASHTO): Washington, DC, USA, 1995.
22. American Society for Testing Materials (ASTM). *D3282-09: Standard Practice for Classification of Soils and Soil-Aggregate Mixtures for Highway Construction Purposes*; ASTM: Pennsylvania, PA, USA, 2009.
23. Jordaan, G.J.; Steyn, W.J.v.M. *Cost-Effective Upgrading of Gravel Roads Using Naturally Available Materials with New-Age Modified Emulsion (Nme) Stabilisation*; Department of Civil Engineering, University of Pretoria: Pretoria, South Africa, 2020; ISBN 978-0-620-91415-4.
24. Asphalt Academy. *Technical Guideline (TG2): Bitumen Stabilised Materials—A Guideline for the Design and Construction of Bitumen Emulsion and Foamed Bitumen Stabilised Materials*; Asphalt Academy c/o CSIR Built Environment: Pretoria, South Africa, 2009.
25. Van Zyl, G.D.; Fourie, H.G. Key aspects of good performing Cape seals. In Proceedings of the 11th Conference on Asphalt Pavements for Southern Africa (CAPSA 2015), Sun City, South Africa, 16–19 August 2015.
26. Jordaan, G.J. Life-cycle cost analysis—An integral part of pavement rehabilitation design. In Proceedings of the 10th Conference on Asphalt Pavements for Southern Africa, Drakensberg, South Africa, 11–14 September 2011.
27. Committee of Land Transport Officials (COLTO). *Standard Specifications for Road and Bridge Works for State Road Authorities*; Civil Engineering Advisory Committee (CEAC): Pretoria, South Africa, 1998.
28. Van Zyl, G.D.; Fourie, H.G.; Bredenhann, S.J. Recommended practice for winter sealing in South Africa. In Proceedings of the 11th Conference on Asphalt Pavements for Southern AFRICA (CAPSA 2015), Sun City, South Africa, 16–19 August 2015.
29. Jordaan, G.J.; Steyn, W.J.v.d.M.; Broekman, A. Evaluation of novel chip seals applications during periods of low temperatures. In Proceedings of the 12th Conference on Asphalt pavements for southern Africa (CAPSA 2019), Sun City, South Africa, 13–16 October 2019.
30. SASOL. *SASOL Wax*; SASOL: Johannesburg, South Africa, 2011.
31. Hurley, G.C.; Powell, B.D. *Evaluation of Sasobit for Use in Warm Mix Asphalt*; NCAT Report 05-06 National Centre for Asphalt Technology; National Centre for Asphalt Technology: Auburn, Alabama, 2005.
32. Wasiuddin, N.M.; Saha, R.; King, W.; Mohammed, L. Effects of Temperature and Shear rate on Viscosity of Sasobit-Modified Binders. *Int. J. Pavement Res. Technol.* **2012**, *5*, 369–378.
33. Jordaan, G.J.; Oerlemans, R.P.; Biekart, H.; Masuku, F.; Kilian, A. Rehabilitation of the N14/1 highway: Use of a modified binder in the asphalt surfacing for construction at low temperatures. In Proceedings of the 11th Conference on Asphalt Pavements for Southern AFRICA (CAPSA 2015), Sun City, South Africa, 16–19 August 2015.
34. SASOL. *Sasobit REDUX—Product Information and Summary of Results*; SASOL: Johannesburg, South Africa, 2016.
35. Sengoz, B.; Topal, A.; Tanyel, A. Comparison of Pavement Surface Texture Determination by Sand Patch Test and 3D Laser Scanning. *Period. Polytech. Civ. Eng.* **2012**, *56*, 73–78. [[CrossRef](#)]
36. American Society for Testing Materials (ASTM). *Standard Practice for Calculating Pavement Macro-Texture Mean Profile Depth*; ASTM E 1845-01; American Society for Testing Materials (ASTM): Pennsylvania, PA, USA, 2003.
37. American Society for Testing Materials (ASTM). *Standard Test Method for Measuring Pavement Macro-Texture Depth Using A Volumetric Technique*; ASTM E 965-96; American Society for Testing Materials (ASTM): Pennsylvania, PA, USA, 2006.